Int. J Solids Structures, 1966, Vol 2, pp 493 to 513 Pergamon Press Ltd Printed in Great Britain

LIMIT ANALYSIS OF CIRCULAR PLATES WITH JUMP NON-HOMOGENEITY

J. A. KÖNIG and J. RYCHLEWSKI

Institute of Fundamental Technical Problems, Polish Academy of Sciences, Warsaw, Poland

Abstract—In many practical problems the need arises to consider bodies whose non-homogeneity is described by non-continuous functions.

The subject of the paper is the determination of the carrying capacity of simply supported circular plates, loaded by uniform pressure and composed of concentric annuli with different mechanical properties. The above jump of mechanical properties may be caused by jump of plate thickness or by change of material properties.

Depending on the values of non-homogeneity and the division parameters there exist six different solutions of the considered problem. In each particular case the moment field, velocity field and limit load are given The ranges of validity of all solutions are established Also, the problem of optimum design in the above class of plates is considered.

In the second part an orthotropic plate is discussed The special case concerning the uniform distribution of circumferential reinforcement in the case of a reinforced concrete plate is considered. Here again, depending on different parameters, there may be seven solutions.

The above analysis has allowed some qualitative conclusions to be drawn concerning the design of isotropic and orthotropic plates with jump non-homogeneity.

1. INTRODUCTION

A CONTINUOUS medium possesses jump non homogeneities if there exist surfaces in which the values of material constants suffer jump changes. This non-homogeneity is described by discontinuous functions. Problems with such jumps constitute a comprehensive class of essential practical importance and also have interesting theoretical aspects.

Recently, the behaviour of an ideally plastic material with a discontinuous distribution of yield limit has been explored, [1]. Papers [2, 3] are devoted to the problems of plane flow, while in [4, 5], the carrying capacity of bars, composed of a number of materials, in torsion has been analysed.

In the present paper we consider some examples of limit analysis of plates with jump non-homogeneity. Within the frame of the theory of limit analysis it is assumed that mechanical properties of plates at generic point are completely defined by the shape of the limit surface in the space of bringing moments M_{11}, M_{22}, M_{12}: $F(M_{\alpha\beta}, C_\nu) = 0$. The plate is called *plate with jump non-homogeneity* if its middle surface may be divided in n regions G_μ with the limit surface being constant inside of each region, but differing on their bounds $F_\mu = 0$.

Very often, but in general not always, the form of the functions F_μ as functions of $M_{\alpha\beta}$ is identical for the whole plate with different constant C_ν for each region G_μ. In this case jump non-homogeneity is described by piece-wise constant functions $C_\nu(x_1, x_2)$, where x_1, x_2 denote the coordinates of the middle surface.

The reasons that two adjacent parts of the plate have different properties may be of various kind. In the simplest case of a plate which is isotropic and homogeneous along its thickness, with the limit surface of the form $F = M_{11}^2 - M_{11}M_{22} + M_{22}^2 + 3M_{12}^2 - M_0^2 = 0$, we have $M_0 = \sigma_0 H^2$ where σ_0 is the yield limit and $2H$ denotes the plate thickness. The jump of M_0 may be produced either by the jump of σ_0 or by the jump of H. The plate with two differenf structures along its thickness gives another example. The jump in reinforcement percentage in the concrete plate is the typical example of jump non-homogeneity in the case of orthotropy.

Our paper is based on usual fundamental assumptions of limit analysis of plates, [6]. Thus the local three-dimensional states of stress and strain in the neighbourhood of contact surface between the parts with various mechanical properties are not taken into account.

2. FORMULATION OF THE PROBLEM

We shall consider the circular plate composed of two concentric parts of various mechanical properties. For instance let us take the simple case when our plate is loaded by a uniform pressure p and simply supported on its circumference, Fig. 1.

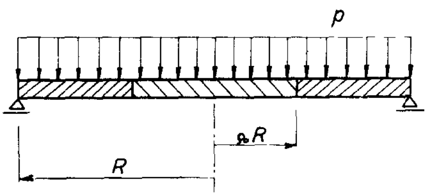

FIG. 1

At the beginning we shall discuss isotropic plates. We assume the validity of a limit relation obtained from the Tresca yield condition

$$F = \max\{|m_r - m_\varphi|, |m_r|, |m_\varphi|\} - f(\rho) = 0 \tag{2.1}$$

where $m_r = M_r/M_0$ and $m_\varphi = M_\varphi/M_0$ are dimensionless radial and circumferential bending moments, respectively, M_0 is the limit moment in the *stronger* part. The associated flow rule takes the form

$$\dot{\varkappa}_r = -\dot{w}'' = \frac{\partial F}{\partial m_r}, \qquad \dot{\varkappa}_\varphi = -\frac{\dot{w}'}{\rho} = \frac{\partial F}{\partial m_\varphi} \tag{2.2}$$

where $\dot{\varkappa}_r$, $\dot{\varkappa}_\varphi$ are curvature velocities multiplied by R^2 (R is the plate radius), ρ denotes the radial coordinate related to R, a prime denotes differentiation with respect to ρ.

The jump non-homogeneity of the plate is described by the function $f(\rho)$. For the plate with the weaker central part we have:

$$f(\rho) = \eta I(0, \rho_0) + I(\rho_0, 1) \tag{2.3}$$

while for the other case:

$$f(\rho) = I(0, \rho_0) + \eta I(\rho_0, 1) \tag{2.4}$$

where

$$0 \leqslant \eta \leqslant 1, \qquad 0 \leqslant \rho_0 \leqslant 1$$

and $I(\alpha, \beta)$ is a function called the rectangular impulse, i.e.

$$I(\alpha, \beta) \equiv H(x-\alpha)-H(x-\beta) \equiv \begin{cases} 0, & x < \alpha \\ 1, & \alpha \leqslant x < \beta, \qquad \alpha < \beta. \\ 0, & \beta \leqslant x \end{cases} \tag{2.5}$$

Here $H(x)$ is the Heaviside function. In these cases, when the purpose of the function $I(\alpha, \beta)$ is not only to shorten the notation and make it clear, we make use of the following obvious relations

$$I(\alpha, \beta) \,.\, I(\gamma, \delta) = I(\gamma, \beta), \qquad \alpha < \gamma < \beta < \delta \tag{2.6}$$

$$\int_0^x f(t) I(\alpha, \beta)\, \mathrm{d}t = I(\alpha, \beta) \int_\alpha^x f(t)\, \mathrm{d}t + I(\beta, 1) \int_\alpha^\beta f(t)\, \mathrm{d}t, \qquad 0 < \alpha < \beta < 1 \tag{2.7}$$

$$\frac{\mathrm{d}}{\mathrm{d}x}[f(x) I(\alpha, \beta)] = f'(x) I(\alpha, \beta) + f(\alpha)\delta(x-\alpha) - f(\beta)\delta(x-\beta) \tag{2.8}$$

where $\delta(x)$ denotes the Dirac function.

The quantity ρ_0 as before will be called the *division parameter*, while the quantity η defining the limit moments ratio is the *non-homogeneity parameter* (Fig. 2). The equilibrium

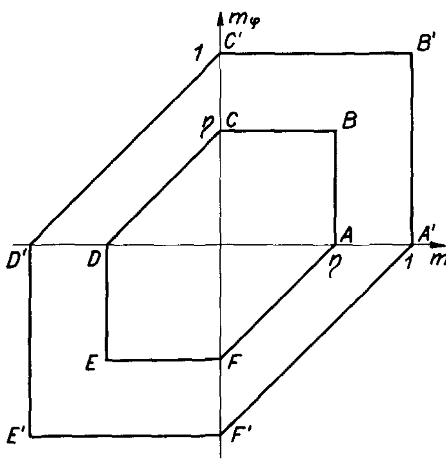

FIG. 2.

equation takes the form:

$$m_r' + \frac{1}{\rho}(m_r - m_\varphi) = -\tfrac{1}{2} q \rho, \qquad q \equiv \frac{pR^2}{M_0} \tag{2.9}$$

and boundary conditions are the following:

$$\rho = 1: \qquad \dot{w} = m_r = 0 \tag{2.10}$$

$$\rho = 0: \qquad m_r = m_\varphi. \tag{2.11}$$

The purpose of the paper is to investigate the influence of parameters ρ_0, η on the carrying capacity and on the kinematics of the beginning of the unconstrained plastic flow of the plate.

In Section 5 the practically important, but more complicated case of the orthotropic plate will be considered.

3. ISOTROPIC PLATE WITH A WEAK INTERNAL PART

When η is close to 1, the solution should be close to the well-known solution for the homogeneous plate, irrespectively of ρ_0. From this remark Solution 1 follows:

Solution 1

We assume that the stress profile is placed on the side BC for the internal part and on the side B′C′ for the external part of the plate e.g.

$$m_\varphi = f(\rho) = \eta I(0, \rho_0) + I(\rho_0, 1) \tag{3.1}$$

The jump of m_φ for $\rho = \rho_0$ is statically admissible. Substituting (3.1) into (2.9) and making use of the second relation (2.11) we obtain

$$m_r = -\frac{q}{6}\rho^2 + \frac{1}{\rho}\int_0^\rho \{\eta I(0, \rho_0) + I(\rho_0, 1)\}\,\mathrm{d}\rho = \left(\eta - \frac{q}{6}\rho^2\right) I(0, \rho_0)$$
$$+\left[1 - \frac{q}{6}\rho^2 - \frac{\rho_0}{\rho}(1-\eta)\right] I(\rho_0, 1). \tag{3.2}$$

The quantity of limit load yields from (2.10),

$$q_1 = 6[1 - \rho_0(1-\eta)]. \tag{3.3}$$

From (2.2), (3.1) we have $\dot{\kappa}_r = 0$ for the whole plate. In this way

$$\dot{w} = \dot{w}_0(1-\rho) \tag{3.4}$$

thus the above kinematics of the destruction coincides with that for a homogeneous plate. For $\rho_0 = 0$ and $\eta = 1$ formulae (3.1), (3.2), (3.3) also gives the known solution.

It is convenient to represent the stress profile in a three-dimensional space of m_r, m_φ, ρ. In this space the limit relation (2.1), (2.3) takes the form of the surface shown in Fig. 3. As before, this surface will be called the *surface of the mechanical properties.*

Now we shall define the bounds of validity of the given solution. It is easy to see that $m_r(\rho)$ decreases monotonically from η (for $\rho = 1$) to 0 (for $\rho = 0$) if

$$2\rho_0^3(1-\eta) - 2\rho_0^2 + (1-\eta) \leqslant 0.$$

For

$$2\rho_0^3(1-\eta) - 2\rho_0^2 + (1-\eta) > 0$$

we have

$$m_r' = 0 \quad \text{for} \quad \rho = \rho_* \equiv \{\rho_0(1-\eta)/2[1-\rho_0(1-\eta)]\}^{\frac{1}{3}} > \rho_0. \tag{3.5}$$

Thus m_r reaches the analytical maximum for $\rho = \rho_*$, $\rho = 0$ and the non-analytical minimum for $\rho = \rho_0$ (Fig. 3).

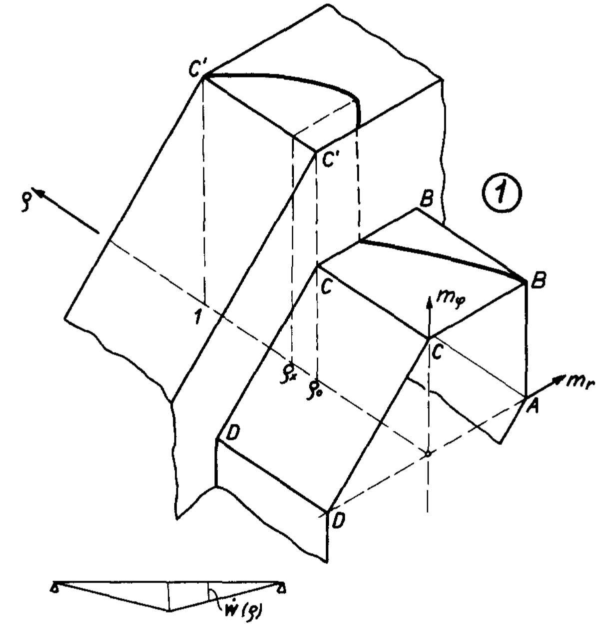

FIG. 3.

It means that η is sufficiently small for the given ρ_0 and the weaker region is partially clamped in the external stronger annulus.

The solution holds when

$$m_r(\rho_0) \geqslant 0, \qquad f_{12} \equiv \eta - (\rho_0^2 - \rho_0^3)/(1-\rho_0^3) \geqslant 0 \tag{3.6}$$

It may be demonstrated that the condition $m_r(\rho_*) \leqslant 1$ is always satisfied.

Solution 2

In the case when the inequality (3.6) is not satisfied, the negative moments m_r appear in both parts of the plate. The stresses in the intervals $(0, \xi_1)$, (ξ_1, ρ_0), (ρ_0, ξ_2), $(\xi_2, 1)$ corresponding to the sides BC, CD, C′D′, B′C′, respectively. It may be written by means of the impulse function in the form of the single function

$$m_\varphi = \eta I(0, \rho_0) + I(\rho_0, 1) + m_r I(\xi_1, \xi_2) \tag{3.7}$$

Substituting (3.7) into the equilibrium equation (2.9), and integrating, taking into account the boundary conditions:

$$m_r(0) = \eta; \qquad m_r(\xi_1) = m_r(\xi_2) = m_r(1) = 0$$

we obtain

$$m_r = \eta\left(1-\frac{\rho^2}{\xi_1^2}\right)I(0,\xi_1) - \eta\left[\frac{3}{2}\left(\frac{\rho^2}{\xi_1^2}-1\right) - \ln\frac{\rho}{\xi_1}\right]I(\xi_1,\rho_0) - \left[\frac{3\eta}{2\xi_1^2}(\rho^2-\xi_2^2) - \ln\frac{\rho}{\xi_2}\right]I(\rho_0,\xi_2)$$
$$+\frac{\eta}{\rho\xi_1^2}(\rho-\xi_2)(1-\rho)(1+\rho+\xi_2)I(\xi_2, 1) \tag{3.8}$$

here the limit load is

$$q_2 = \frac{6\eta}{\xi_1^2}. \tag{3.9}$$

The coordinates ξ_1, ξ_2 describing the range of negative moments are defined by the system of equations:

$$\xi_1^2 = (1+\xi_2+\xi_2^2)\eta \tag{3.10}$$

$$\frac{3}{2}\eta\left(1-\frac{\xi_2^2}{\xi_1^2}\right)+\ln\frac{\xi_2}{\rho_0}-\eta\ln\frac{\xi_1}{\rho_0} = 0. \tag{3.11}$$

The stress profile on the surface of mechanical properties is shown in Fig. 4.

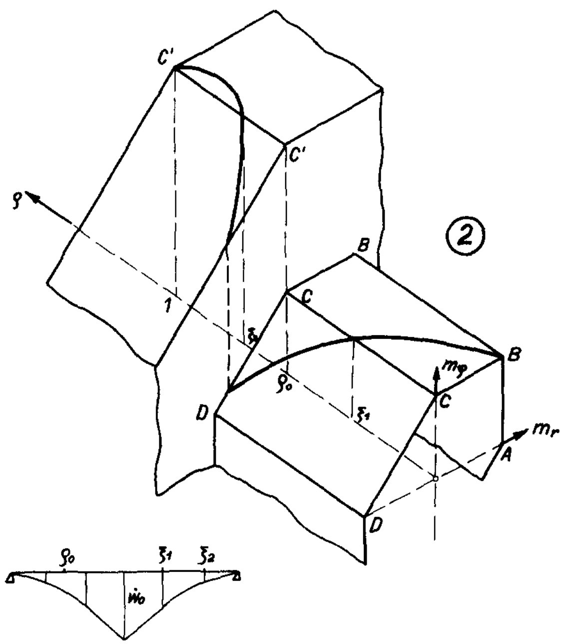

FIG. 4.

From (2.2), (3.7) we obtain that $\dot{\varkappa}_r = 0$ in the intervals $(0, \xi_1)$, $(\xi_2, 1)$ and that $\dot{\varkappa}_r+\dot{\varkappa}_\varphi = 0$ for (ξ_1, ξ_2). This may be written as follows:

$$\dot{w}''+\frac{1}{\rho}I(\xi_1, \xi_2)\dot{w}' = 0. \tag{3.12}$$

Integrating this equation we have:

$$\dot{w} = \dot{w}_0-w_0c\left\{\frac{\rho}{\xi_1}I(0, \xi_1)+\left(1+\ln\frac{\rho}{\xi_1}\right)I(\xi_1, \xi_2)+\left(\ln\frac{\xi_2}{\xi_1}+\frac{\rho}{\xi_2}\right)I(\xi_2, 1)\right\}. \tag{3.13}$$

From the boundary condition $\dot{w}(1) = 0$ we obtain

$$c = \xi_2/\left(1+\xi_2\ln\frac{\xi_2}{\xi_1}\right).$$

It is easy to see that $\dot{w}'$ is continuous, $\dot{w}''$ possesses jumps and at that δ-functions† are involved in $\dot{w}'''$.

Now we shall define the bound of validity of the given solution. Thus $m_r(\rho)$ reaches the analytical maximum for

$$\rho = \rho_* \equiv (\xi_2 + \tfrac{1}{2}\xi_2^2)^{\frac{1}{3}} > \xi_2, \qquad \rho = 0$$

and the non-analytical minimum for $\rho = \rho_0$, Fig. 4. The validity region is defined by the next conditions

$$m_r(\rho_0) \leqslant 0, \qquad f_{12} \leqslant 0, \tag{3.14}$$

$$\xi_2 \leqslant 0, \qquad f_{23} \equiv \ln \rho_0 - [\eta(3 - \ln 3\eta) - 1]/2(1-\eta) \geqslant 0, \tag{3.15}$$

$$m_r(\rho_0) \geqslant -\eta, \qquad \ln \frac{\rho_0^2}{\xi_1^2} - 3\frac{\rho_0^2}{\xi_1^2} + 5 \geqslant 0, \; f_{24} \equiv \xi_1(\eta, \rho_0) - 0{\cdot}73\rho_0 \geqslant 0, \tag{3.16}$$

where $\xi_1(\eta, \rho_0)$ is expressed by (3.10–11). The condition $m_r(\rho_*) < 1$ is always satisfied.

Solution 3

When the inequality (3.15) is not satisfied, the range with the negative moment m_r extends on the whole to the stronger part of the plate. Then

$$m_\varphi = \eta I(0, \rho_0) + I(\rho_0, 1) + m_r I(\xi_1, 1) \tag{3.17}$$

Using the equilibrium equation and the boundary conditions $m_r(0) = \eta, m_r(\xi_1) = m_r(1) = 0$ we have

$$m_r = \eta\left(1 - \frac{\rho^2}{\xi_1^2}\right) I(0, \xi_1) - \eta\left[\frac{3}{2}\left(\frac{\rho^2}{\xi_1^2} - 1\right) - \ln\frac{\rho}{\xi_1}\right] I(\xi_1, \rho_0) - \left[\frac{3\eta}{2\xi_1^2}(\rho^2 - 1) - \ln\rho\right] I(\rho_0, 1) \tag{3.18}$$

where the parameter ξ_1 is defined by the relation

$$\eta \ln\frac{1}{\xi_1} - \frac{3\eta}{2}\frac{1}{\xi_1^2} + \frac{3\eta}{2} + (\eta - 1)\ln\rho_0 = 0 \tag{3.19}$$

and the limit load is expressed by formula (3.9). It is easy to see that relations (3.17), (3.18), (3.19), can be obtained from (3.7), (3.8), (3.11), if we set $\xi_2 = 1$. Similarly, the velocity field is given by:

$$\dot{w} = \dot{w}_0 - \dot{w}_0 c\left\{\frac{\rho}{\xi_1} I(0, \xi_1) + \left(1 + \ln\frac{\rho}{\xi_1}\right) I(\xi_1, 1)\right\}, \qquad c = 1/(1 - \ln \xi_1). \tag{3.20}$$

The bounds of validity for the solution are as follows:

$$m_r'(1) \geqslant 1, \qquad f_{23} \leqslant 0, \tag{3.21}$$

$$m_r(\rho_0) \geqslant -\eta, \qquad f_{24} \leqslant 0, \qquad \eta \geqslant \rho_0^2 \ln \rho_0/(1{\cdot}815\rho_0^2 - 2{\cdot}815). \tag{3.22}$$

In the last condition the relation (3.19) has been used.

Solution 4

Let the division parameter ρ_0 in the solutions 2 and 3 be chosen. For a certain value

† The interval $(0, \alpha)$ is understood as $(-\varepsilon, \alpha)$ and the interval $(\alpha, 1)$, as $(\alpha, 1+\varepsilon)$ where $\varepsilon > 0$. It leads to relations:

$$I(0, \alpha) = \delta(x) - \delta(x - \alpha) = -\delta(x - \alpha) \quad \text{for} \quad 0 \leqslant x \leqslant 1.$$

$\eta = \eta^*$ in (3.16) an equality occurs (for the solution 2) or (3.22) (for the solution 3). It corresponds to the case when

$$m_r(\rho_0) = -\eta^*, \qquad \xi_1^* = 0{\cdot}73\rho_0, \qquad \eta = \eta^*(\rho_0) \tag{3.23}$$

thus the state D is realized on the contact annulus (see Figs. 2 and 4). In this case the rates $\dot{\varkappa}_r$, $\dot{\varkappa}_\varphi$ are not unique for $\rho = \rho_0$ in (2.2). In other words, for $\eta = \eta^*$ the *plastic hinge* on $\rho = \rho_0$ may develop. The hinge appears in the weaker part near the contact annulus.

A further decreasing of η leads to a new destruction scheme with the plastification of the weaker part only. That part will behave then as a clamped one in the *rigid external annulus* (see Fig. 5).

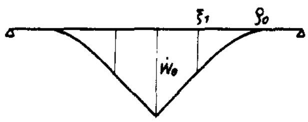

FIG. 5.

For this case we obtain the stress profile $m_r(\rho)$, $m_\varphi(\rho)$ from the profiles (3.7), (3.8) setting $\eta = \eta^*$, $\xi_2 = \xi_2^*$ and decreasing the scale, e.g.

$$\begin{aligned} m_r &= \frac{\eta}{\eta^*} m_r^{(2)}(\rho, \eta^*, \xi_1^*, \xi_2^*), \\ m_\varphi &= \frac{\eta}{\eta^*} m_\varphi^{(2)}(\rho, \eta^*, \xi_1^*, \xi_2^*) \end{aligned} \tag{3.24}$$

for $f_{23} \leqslant 0$. The terms with $I(0, \xi_1^*)$, $I(\xi_1^*, \rho_0)$ describe then the known solution for the clamped plate with the radius $\rho_0 R$, instead of the terms with $I(\rho_0, \xi_2^*)$, $I(\xi_2^*, 1)$ which describe the extrapolation of the stress profile into the rigid part. This extrapolation lies inside the surface of the mechanical properties.

In the same way we have

$$m_r = \frac{\eta}{\eta^*} m_r^{(3)}(\rho, \eta^*, \xi_1^*), \qquad m_\varphi = \frac{\eta}{\eta^*} m_\varphi^{(3)}(\rho, \eta^*, \xi_1^*) \tag{3.25}$$

for $f_{23} \geqslant 0$.

The profiles (3.24), (3.25) differ one from the other in the extrapolation only.

The limit load is:

$$q_4 = 11{\cdot}26\frac{\eta}{\rho_0^2}. \tag{3.26}$$

Making use of (2.2), (3.24) and of the condition $\dot{w}'(\rho_0) = 0$ we obtain the kinematic of the initial motion in the following form:

$$\dot{w} = \dot{w}_0\left\{\left(1 - c\frac{\rho}{\xi_1}\right)I(0, \xi_1) + \left[1 - c\left(1 + \ln\frac{\rho}{\xi_1}\right)\right]I(\xi_1, \rho_0)\right\} \tag{3.27}$$

where $c = 1/(1 + \ln \rho_0/\xi_1)$ (Fig. 5). Using formula (2.8) we see that $\dot{w}'$ is a step function, while

$$\dot{w}'' = \frac{\dot{w}_0 c}{\rho^2} I(\xi_1, \rho_0) + \frac{\dot{w}_0 c}{\rho_0} \delta(\rho - \rho_0). \tag{3.28}$$

The function of Dirac appearing in this equation represents the plastic hinge; it provides the infinite value of the rate of change of radial curvature. When we use a notation of this kind there is no need for separate consideration of plastic hinges, e.g. in the case of calculating the power of dissipation.

The complete set of all solutions is represented in Fig. 6.

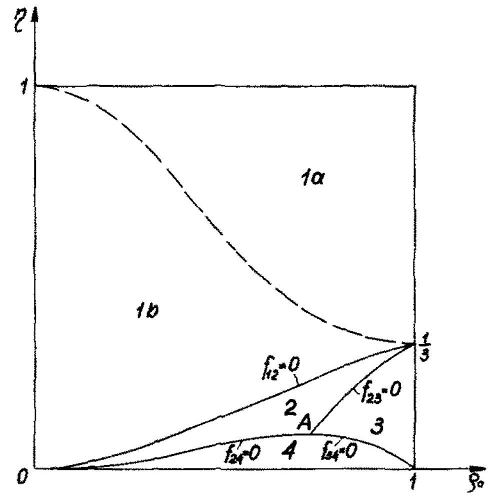

FIG 6.

It is easy to see that in each case there exists a continuous transition of all functions and quantities through all division lines between the regions of validity of the solutions.

The lines $\eta = 1$, $\rho_0 = 0$ correspond to the homogeneous plate with the limit moment equal to M_0.

The line $\rho_0 = 1$ corresponds to the homogeneous plate with the limit moment ηM_0. The dotted line dividing the region 1 corresponds to $m_r'(\rho_0) = 0$.

The determination of the bound of the region 4, $f_{24}(\eta, \rho_0) = 0$, $f_{34}(\eta, \rho_0) = 0$, seems to be the most important aspect resulting from the solution. For the values of division parameter ρ_0 and non-homogeneity parameter η lying above these lines, both parts of the plate in the limit state work together. For ρ_0, η below them only the central part flows in the limit state; therefore the material in the circumferential annulus is not entirely exhausted. An engineering aspect of the remark is the following: when the stronger part is designed as the clamped ring for the central plate, the selection of the division parameter ρ_0 defines uniquely the smallest requisite ratio of limit moment of the annulus to the plate limit moment, $\eta = \eta^*$.

One can make two qualitative observations which can be deduced from Fig. 6. For every ρ_0:

(a) if $\eta \geqslant \frac{1}{3}$, then the radial moments in the plate do not exist,

(b) if $\eta \geqslant \eta_A \approx \frac{1}{11}$ both parts of the plate collaborate in the limit state.

4. ISOTROPIC PLATE WITH A STRONGER CENTRAL PART

In this case the description of the plate behaviour is simpler than that in Section 3.

Solution 1

Similarly as in Section 3, we assume that the stress profile of m_r, m_φ corresponds to sides B′C′, BC. Then

$$m_\varphi = I(0, \rho_0) + \eta I(\rho_0, 1). \tag{4.1}$$

Substituting the relation into the equilibrium equation, integrating, and taking into account the boundary conditions $m_r(0) = 1$, $m_r(1) = 0$, we obtain:

$$m_r = \left\{1 - \rho^2\left[\eta + \rho_0(1-\eta)\right]\right\} I(0, \rho_0) + \frac{\eta + \rho_0(1-\eta)}{\rho}(1-\rho)\left[\rho^2 + \rho + \frac{\rho_0(1-\eta)}{\eta + \rho_0(1-\eta)}\right] I(\rho_0, 1) \tag{4.2}$$

and the limit load:

$$q_1 = 6[\eta + \rho_0(1-\eta)]. \tag{4.3}$$

The velocity field is described by formula (3.4). For $\eta = 1$ or $\rho_0 = 0$ the obtained relations which are identical to those for a homogeneous plate with limit moments M_0 and ηM_0, respectively.†

The analysis of (4.2) shows that m_r is a monotonically decreasing function of ρ. The validity region of the solution is bounded by one condition only (see Fig. 7):

$$m_r(\rho_0) \leqslant \eta M_0, \qquad \eta \geqslant \eta^*(\rho_0) \equiv (1-\rho_0^3)/(1+\rho_0^2-\rho_0^3) \tag{4.4}$$

Solution 2

When for a fixed ρ_0 the non-homogeneity parameter decreases to $\eta = \eta^*$, then on $\rho = \rho_0$ we have $m_r = \eta M_0$ (point B′ on Fig. 7) and the plastic hinge may develop.

For $\eta < \eta^*$ the kinematical scheme relates to the motion of the stronger part as a rigid body.

The external weaker part is plasticised, behaving as an annular plate clamped in vertically movable internal bound $\rho = \rho_0$, loaded by the perpendicular pressure P and by the annulus of shear force

$$q_r = \frac{p\rho_0^2 R^2}{2} \quad \text{on} \quad \rho = \rho_0.$$

The solution takes the form:

$$m_r = \frac{\eta}{\eta^*} m_r^{(1)}(\rho, \eta^*), \qquad m_\varphi = \frac{\eta}{\eta^*} m_\varphi^{(1)}(\rho, \eta^*) \tag{4.5}$$

† For the case $\rho_0 = 0$ the point $\rho = 0$ is evidently a singular point.

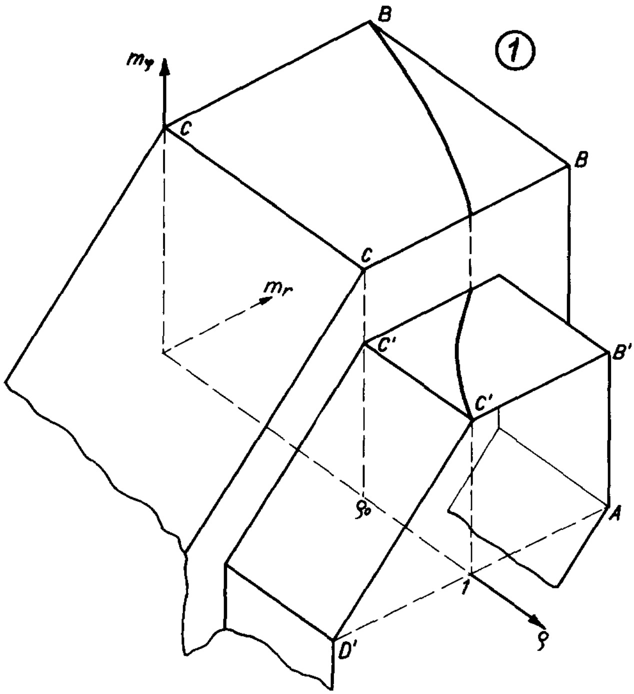

FIG. 7.

where the terms with $I(0, \rho_0)$ represent the stress profile extrapolation into the rigid region and lying inside of the mechanical properties surface.

The limit load is equal to

$$q_2 = \frac{6\eta M_0}{(1-\rho_0^3)} \tag{4.6}$$

and the velocity field is described by formula

$$\dot{w} = \dot{w}_0 I(0, \rho_0) + \dot{w}_0 \frac{1-\rho}{1-\rho_0} I(\rho_0, 1) \tag{4.7}$$

The bounds of validity for the above solutions are given in Fig. 8. The region without collaboration is bigger than for the case in Fig. 6. The bounding lines agree with our intuition.

Finally, let us consider the simple example of the optimization of ρ_0, η parameters. In Section 1 we have considered that the plate with a jump in its thickness is a particular case of a plate with a jump of non-homogeneity.

In this case we have

$$\eta = \frac{h_-^2}{h_+^2}, \qquad h(\rho) = h_+ I(0, \rho_0) + h_- I(\rho_0, 1). \tag{4.8}$$

Let us formulate the extremal problem as follows: in the considered class of plates with volume V_0 we seek the plate with the largest carrying capacity. It is evident that its limit behaviour is described by the solution 1, Section 4.

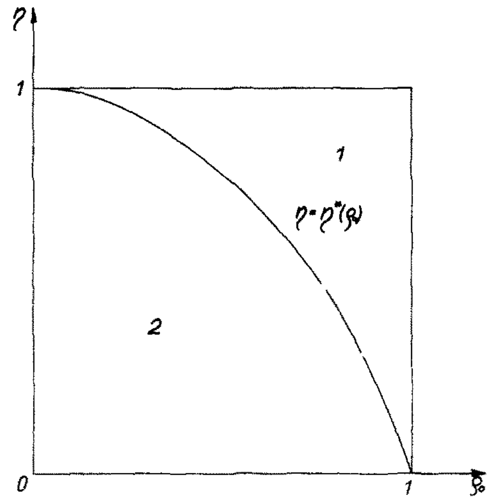

FIG. 8.

For comparison we introduce the plate of constant thickness and volume V_0. Its thickness is $h_e = h_+[\rho_0^2+\eta^{\frac{1}{2}}(1-\rho_0^2)]$ and the limit load is

$$q_e = 6[\rho_0^2+\eta^{\frac{1}{2}}(1-\rho_0^2)], \qquad M_0 = \tfrac{1}{4}\sigma_0 h_+^2. \tag{4.9}$$

We denote by

$$Q\,(\rho_0, \eta) \equiv \frac{q_1}{q_e} = \frac{\eta+\rho_0(1-\eta)}{\rho_0^2+\eta^{\frac{1}{2}}(1-\rho_0^2)} \tag{4.10}$$

the ratio of the limit loads for jump non-homogeneity plate and for the above one.

In such a way the problem is reduced to the determination of

$$\sup Q(\rho_0, \eta), \qquad (\rho_0, \eta) \in D$$

where D is the closed region of validity of the solution 1. It is easy to see that

$$Q(0, \eta) \equiv Q(\rho_0, 1) \equiv 1 \quad \text{and} \quad \frac{\partial Q}{\partial \eta} < 0 \quad \text{for} \quad 0 < \rho_0, \eta < 1. \tag{4.11}$$

It means that $\sup Q(\rho_0, \eta)$ is reached on the bounding line l:

$$\eta = \eta^*(\rho_0) = (1-\rho_0^3)/(1-\rho_0^3+\rho_0^2).$$

Substituting the value of η into (4.10) we have

$$Q|_l = [\rho_0^2(1+\rho_0^2-\rho_0^3)^{\frac{1}{2}}+(1-\rho_0^2)(1-\rho_0^3)^{\frac{1}{2}}]. \tag{4.12}$$

The consideration of the maximum of the function F leads to the next optimal values of parameter

$$\rho_0 \approx 0{\cdot}79, \qquad \eta \approx 0{\cdot}45, \qquad \frac{h_-}{h_+} \approx 0{\cdot}67 \tag{4.13}$$

Substituting them into (4.10) we get:

$$\sup Q(\rho_0, \eta) \approx 1{\cdot}15, \qquad (\rho_0, \eta) \in D. \tag{4.14}$$

Thus the simplest form of the advantageous redistribution of the material in a plate containing one change of the thickness increases the carrying capacity by 15 per cent.

5. ORTHOTROPIC PLATE WITH JUMP NON-HOMOGENEITY

The consideration of orthotropic plates with jump non-homogeneity is of practical importance. Many examples of such kind are given by reinforced concrete plates.

We shall consider now the circular plate composed of two concentric parts. Limit relations for both parts have been presented in Fig. 9. Next M_0 denotes the circumferential limit moment for the *internal* part.

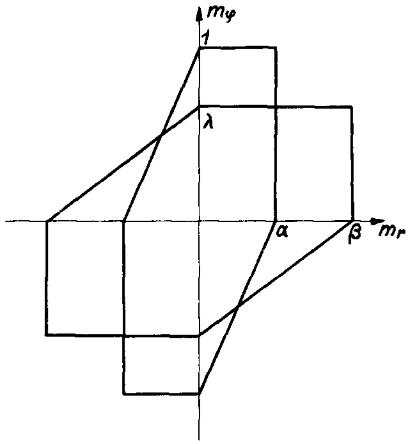

FIG. 9.

The limit condition for the whole plate takes the form:

$$F \equiv \max\left\{\left|\frac{M_\varphi}{f}\right|, \left|\frac{M_r}{g}\right|, \left|\frac{M_r}{g}-\frac{M_\varphi}{f}\right|\right\} - M_0 = 0 \tag{5.1}$$

where the non-homogeneity functions are described as follows:

$$f(\rho) = I(0, \rho_0)+\lambda I(\rho_0, 1), \qquad g(\rho) = \alpha I(0, \rho_0)+\beta I(\rho_0, 1). \tag{5.2}$$

Parameter ρ_0 has the meaning defined in Section 2, parameter λ defines the jump of the circumferential limit moment. The orthotropy coefficients for internal and external parts are $\alpha, \beta/\lambda$, respectively. Thus it seems that our problem is characterized by four independent dimensionless parameters

$$\rho_0: \qquad \lambda, \alpha, \beta. \tag{5.3}$$

The number of their combinations having practical meaning is considerable. In this paper we shall investigate only the particular case

$$\lambda = 1, \qquad 0 \leqslant \alpha, \beta \leqslant 1. \tag{5.4}$$

As it will be seen, the cases $\alpha, \beta > 1$ are also considered. The equality $\lambda = 1$ means (for reinforced concrete) that the circumferential reinforcement is uniformly distributed in the radial direction.

Solution 1

For some variation ranges of ρ_0, α, β parameters ρ_0, β characterizing the jump non-homogeneity have no influence on the limit state. The solution for this case is well known, [7], and may be written in the form:

$$m_\varphi = \left(\alpha+\frac{q}{2}\rho^2\right)I(0,\xi)+I(\xi,1) \tag{5.5}$$

$$m_r = \alpha I(0,\xi)+\left[\left(\frac{1}{\rho}-\rho^2\right)\frac{q}{6}-\left(\frac{1}{\rho}-1\right)\right]I(\xi,1). \tag{5.6}$$

The stress profile on the mechanical properties surface is represented in Fig. 10. The limit load is

$$q_1 = \frac{2(1-\alpha)}{\xi^2} \tag{5.7}$$

where the parameter ξ may be obtained from the equation

$$2(1-\alpha)\xi^3-3\xi^2+(1-\alpha) = 0. \tag{5.8}$$

The second term in m_r monotonically decreases with ρ and $m_r'(\xi) = 0$. The conditions bounding the validity of the solution have the form (compare with Fig. 10)

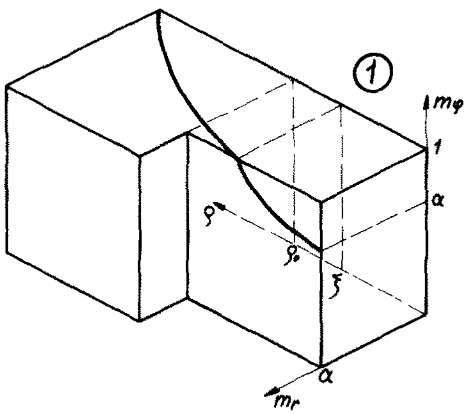

FIG. 10

$$\xi \leqslant \rho_0 \quad (\text{for } \alpha < \beta), \qquad f_{12} \equiv \alpha-\alpha^* \geqslant 0, \qquad \alpha^* \equiv \frac{2\rho_0^3-3\rho_0^2+1}{2\rho_0^3+1} \tag{5.9}$$

$$m_r(\rho_0) \leqslant \beta \quad (\text{for } \alpha > \beta), \qquad f_{14} \equiv \beta-\left(\frac{1}{\rho_0}-\rho_0^2\right)\frac{1-\alpha}{3\xi^2}+\left(\frac{1}{\rho_0}-1\right) \geqslant 0. \tag{5.10}$$

Solution 2

When the parameter α in the solution 1 decreases to α^*, then ξ increases to ρ_0.

The stress profile for the central part must remain on the side $m_r = \alpha$, while the stress profile for the external part is on the side $m_\varphi = 1$. It leads uniquely to the situation shown in Fig. 11. The jump of m_φ on $\rho = \rho_0$ is associated with the jump of the first derivative m'_r,

$$\rho_0 m'_r]_{\rho_0} = m_\varphi]_{\rho_0} \qquad \text{i.e.} \qquad m'_r(\rho_0+0) = \frac{1-m_\varphi(\rho_0-0)}{\rho_0} \tag{5.11}$$

and thus the moment m_r increases beginning with $\rho = \rho_0$. Setting $\xi = \rho_0$ in (5.5), (5.6) we obtain the formulae for m_r, m_φ. The limit load is

$$q_2 = \frac{6[1-\rho_0(1-\alpha)]}{1-\rho_0^3}. \tag{5.12}$$

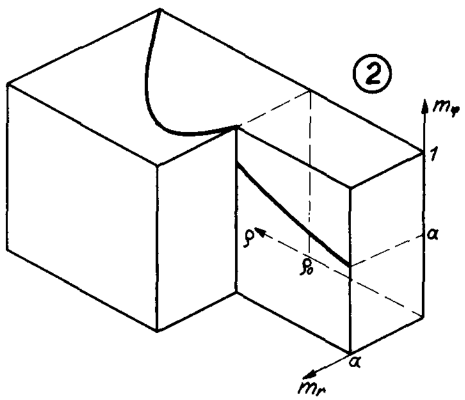

FIG. 11.

The radial moment m_r is extremal for

$$\rho = \rho_* \equiv \frac{\rho_0[(1-\alpha)-\rho_0^2]}{2[1-\rho_0(1-\alpha)]}.$$

The range of validity is defined by the conditions:

$$\rho_* \geqslant \rho_0, \qquad f_{12}(\alpha, \rho_0) \leqslant 0, \tag{5.13}$$

$$m_\varphi(\rho_*) \leqslant \beta, \qquad f_{23} \equiv \beta - 1 + 3\cdot 2^{-\frac{2}{3}}(1-\rho_0^3)^{-1}[1-\rho_0(1-\alpha)]^{\frac{1}{3}}[(1-\alpha)-\rho_0^2]^{\frac{2}{3}}\rho_0^{\frac{4}{3}} \geqslant 0. \tag{5.14}$$

Solution 3

The analysis of statics and kinematics of the plate shows that if the inequality (5.14) is not satisfied, then the state $m_r = \beta$ is realized in one part of the plate. The stress profile assumes the form:

$$m_\varphi = \left(\alpha+\frac{q}{2}\rho^2\right)I(0,\rho_0)+\left(\beta+\frac{q}{2}\xi_1^2\right)I(\rho_0,\xi_1)+\left(\beta+\frac{q}{2}\rho^2\right)I(\xi_1,\xi_2)+I(\xi_2,1), \tag{5.15}$$

$$m_r = \alpha I(0,\rho_0)+\left[\beta+\frac{q\xi_1^2}{6}\left(3-\frac{\rho^2}{\xi_1^2}-2\frac{\xi_1}{\rho}\right)\right]I(\rho_0,\xi_1)+\beta I(\xi_1,\xi_2)+\left[\left(\frac{1}{\rho}-\rho^2\right)-\left(\frac{1}{\rho}-1\right)\right]I(\xi_2,1) \tag{5.16}$$

and the location on the mechanical properties surface is given in Fig. 12.

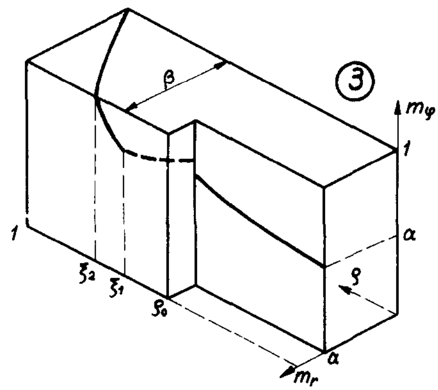

Fig. 12.

The terms with $I(\rho_0, \xi_1)$ represent its part lying inside this surface and constitute the extrapolation of the stress field into the rigid range.

The limit load is given by the formula:

$$q_3 = \frac{2(1-\beta)}{\xi_2^2} \tag{5.17}$$

where the coordinates ξ_1, ξ_2 are defined by the system of equations

$$2(1-\beta)\xi_2^3 - 3\xi_2^2 + (1-\beta) = 0, \tag{5.18}$$

$$2\xi_1^3 - 3\xi_1^2 + \rho_0^3 - \frac{6(\beta-\alpha)}{q}\rho_0 = 0. \tag{5.19}$$

The range of validity is defined by the conditions:

$$\xi_1 \geqslant \rho_0, \qquad f_{35} \equiv \beta - \alpha \geqslant 0, \tag{5.20}$$

$$\xi_2 \geqslant \xi_1, \qquad f_{23} \leqslant 0. \tag{5.21}$$

Solution 4

If the parameter β in the solution 1 decreases and the remaining parameters are constant, then the stress profile takes the form as in the Fig. 13 and is described by formulae:

$$m_\varphi = \left(\alpha + \frac{q}{2}\rho^2\right) I(0, \xi_1) + \left(\alpha + \frac{q}{2}\xi_1^2\right) I(\xi_1, \rho_0) + I(\rho_0, 1) \tag{5.22}$$

$$m_r = \alpha I(0, \xi_1) + \left[\alpha - \frac{q\xi_1^2}{6}\left(\frac{\rho^2}{\xi_1^2} + 2\frac{\xi_1}{\rho} - 3\right)\right] I(\xi_1, \rho_0) + \left[\frac{\rho_0}{\rho}\beta + \left(1 - \frac{\rho_0}{\rho}\right) - \frac{q\rho^2}{6}\left(1 - \frac{\rho_0^3}{\rho^3}\right)\right] I(\rho_0, 1). \tag{5.23}$$

The terms with $I(\xi, \rho_0)$ represent the profile part located inside the surface of the mechanical properties. The limit load is defined by formula (5.7); here α must be replaced by β. The coordinates ξ_1 can be determined from the equation (5.8) but α and β must be interchanged.

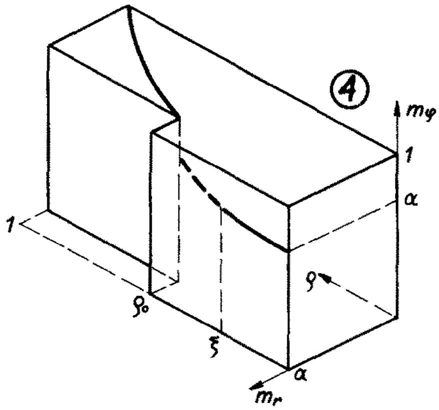

FIG. 13.

The solution is valid when the following conditions are satisfied:

$$m_\varphi(\rho_0)] \geqslant 0, \qquad f_{14} \leqslant 0, \tag{5.24}$$

$$m_r'(\rho_0+0) \leqslant 0, \qquad f_{45} \equiv \beta-\beta^* \geqslant 0, \qquad \beta^* \equiv \alpha^*, \tag{5.25}$$

$$\xi_1 \geqslant 0, \qquad f_{46} \equiv \beta-(1-\rho_0^3)\alpha-\rho_0^2(\rho_0-1) \geqslant 0. \tag{5.26}$$

Solution 5

When the condition (5.20) is not satisfied, then in the external part the region with $m_r = \beta$ appears. The stress profile is described by the relations:

$$m_\varphi = \left(\alpha+\frac{q}{2}\rho^2\right)I(0, \xi_1)+\left(\alpha+\frac{q}{2}\xi_1^2\right)I(\xi_1, \rho_0)+\left(\beta+\frac{q}{2}\rho^2\right)I(\rho_0, \xi_2)+I(\xi_2, 1) \tag{5.27}$$

$$m_r = \alpha I(0, \xi_1)+\left[\alpha-\frac{q\xi_1^2}{2}\left(\frac{\rho^2}{\xi_1^2}+2\frac{\xi_1}{\rho}-3\right)\right]I(\xi_1, \rho_0)+\beta I(\rho_0, \xi_2)$$
$$+\left[1-\frac{1-\beta}{3}\left(2\frac{\xi_2}{\rho}+\frac{\rho^2}{\xi_2^2}\right)\right]I(\xi_2, 1). \tag{5.28}$$

The limit load is given by (5.17), the coordinate ξ_2 by (5.18), ξ_1 is determined from formula (5.19) with α and β interchanged.

The validity region is defined by the following conditions:

$$\xi_1 \leqslant \rho_0, \qquad f_{35} \equiv \beta-\alpha \leqslant 0, \tag{5.29}$$

$$\xi_2 \geqslant \rho_0, \qquad f_{45} \equiv \beta-\beta^* \leqslant 0, \tag{5.30}$$

$$\xi_1 \geqslant 0, \qquad f_{57} \equiv \beta-1+3\cdot 2^{-\frac{1}{3}}\rho_0^{-2}(\alpha-\beta)^{\frac{1}{3}}[\rho_0^2-(\alpha-\beta)]^{\frac{2}{3}} \geqslant 0. \tag{5.31}$$

Solution 6

When in the solution 4 the coordinate ξ_1 tends to 0, then the part of the stress profile of the internal annulus lying inside of the surface of mechanical properties becomes larger and larger. Beginning with $\xi = 0$, the parameter α has no effect on the solution.

The stress profile is described by the following formulae:

$$m_\varphi = \left(\beta+\frac{q\rho_0^2}{6}\right)I(0,\rho_0)+I(\rho_0,1), \tag{5.32}$$

$$m_r = \left[\beta+\frac{q\rho_0^2}{6}\left(1-\frac{\rho^2}{\rho_0^2}\right)\right]I(0,\rho_0)+\left[\left(\frac{1}{\rho}-1\right)+\frac{q}{6}\left(\frac{1}{\rho}-\rho^2\right)\right]I(\rho_0,1), \tag{5.33}$$

where the quantity q is defined by (5.12). The shape of the stress profile is shown in Fig. 14.

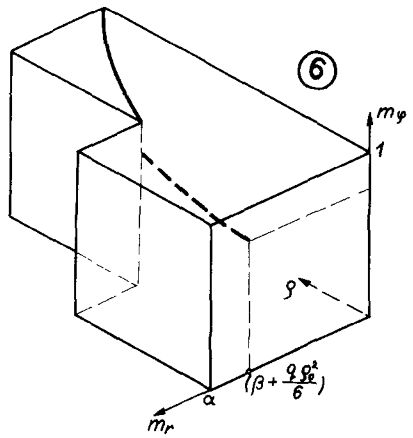

FIG. 14.

The region of validity for the solution is defined by the conditions:

$$m_r(0) \leqslant \alpha, \qquad f_{46} \leqslant 0, \tag{5.34}$$

$$m_r'(\rho_0+0) \leqslant 0, \qquad f_{67} \equiv f_{45} \equiv \beta-\beta^* \geqslant 0. \tag{5.35}$$

Solution 7

This solution results from the solution 6 when the condition (5.35) is not satisfied, or from the solution 5 when the condition (5.31) is not satisfied. The stress profile, given in Fig. 15 is described by the formulae:

$$m_\varphi = \left(\beta+\frac{q\rho_0^2}{6}\right)I(0,\rho_0)+\left(\beta+\frac{q\rho^2}{2}\right)I(\rho_0,\xi_2)+I(\rho_0,1) \tag{5.36}$$

$$m_r = \left[\beta+\frac{q\rho_0^2}{6}\left(1-\frac{\rho^2}{\rho_0^2}\right)\right]I(0,\rho_0)+\beta I(\rho_0,\xi_2)+\left[1-(1-\beta)\frac{\xi_2}{\rho}-\frac{q\xi_2^2}{6}\left(\frac{\xi_2}{\rho}-\frac{\rho^2}{\xi_1^2}\right)\right]I(\rho_0,1) \tag{5.37}$$

where the coordinate ξ_2 is defined by the equation (5.18), and the limit load q by formula (5.17).

The solution 7 is valid if the conditions:

$$m_r(0) \leqslant \alpha, \qquad f_{57} \leqslant 0, \tag{5.38}$$

$$\xi_2 \geqslant \rho_0, \qquad f_{67} \leqslant 0, \tag{5.39}$$

hold.

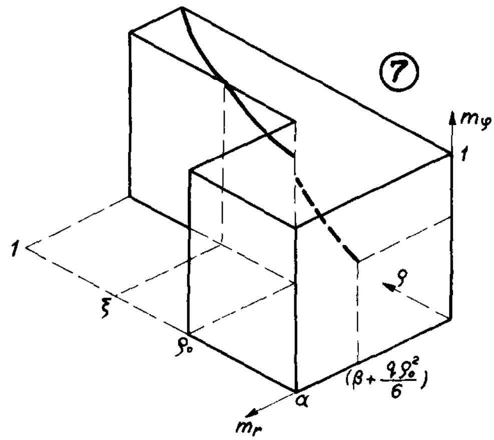

FIG 15.

The kinematics of the beginning of unconstrained plastic flow is described by the formula

$$\dot{w} = \dot{w}_0 I(0, t) + \dot{w}_0 \frac{1-\rho}{1-t} I(t, 1) \tag{5.40}$$

where t is equal to ξ for solution 1, ρ_0 for solution 2, 4, 6, ξ_2 for solutions 3, 5, 7. The coordinate $\rho = t$ defines the location of the plastic hinge. For the solutions 2, 4, 6, the hinge develops on the contact annulus where the jump of the mechanical properties of the plate exists.

In the C_3 space of the ρ_0, α, β parameters the surfaces

$$f_{12} = 0, \quad f_{14} = 0, \quad f_{23} = 0, \quad f_{35} = 0, \quad f_{45} = 0, \quad f_{46} = 0, \quad f_{57} = 0, \quad f_{67} = 0 \tag{5.41}$$

separate the cube $0 \leqslant \alpha;\ \beta,\ \rho_0 \ \leqslant 1$ into seven regions of validity of the derived solutions.

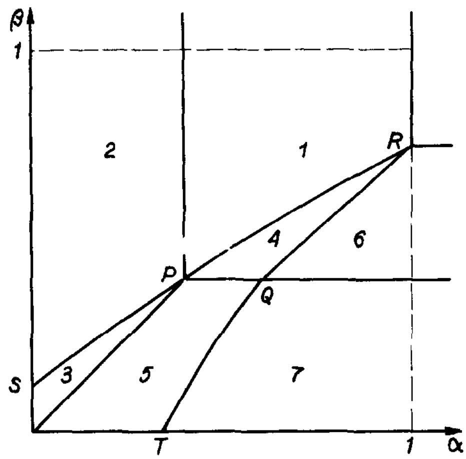

FIG. 16.

The nature of the division is schematically shown in Fig. 16.

When $\rho_0 \to 1$ then $R \to \{1, 0\}$; $S, P \to \{0, 0\}$; $T, Q \to \{\frac{1}{3}, 0\}$

When $\rho_0 \to 0$ then $P, Q, R \to \{1, 1\}$; $T \to \{0, 0\}$; $S \to \{0, 1\}$.

Constructing the above solutions we assumed that $\alpha, \beta \leqslant 1$. In fact, these restrictions are not essential. It is easy to see that the solutions 1, 2 adjacent to the line $\beta = 1$ are independent of β (compare Figs. 10 and 11) and are valid also for $\beta > 1$.

Similarly, the solutions 6 and 7 do not depend on α and are valid for $\alpha > 1$. For the case $\alpha > 1$, $\beta > \beta_R$ the classical solution for an isotropic, homogeneous plate is valid. This solution can be obtained from the solution 1 for $\alpha = 1$.

We have given the complete analysis of the case of $\lambda = 1$. This assumption gives the solutions without negative radial moments m_r. When $\lambda \neq 1$ (e.g. the jump of the circumferential limit moment can exist) the regions with $m_r < 0$ may develop as for the isotropic plate (see Sections 2, 3, 4).

REFERENCES

[1] J. RYCHLEWSKI, Plastic jump non-homogeneity. *Bull. Acad. polon. Sci. Sér. Sci. tech.* **12,** 341 (1964).
[2] J. RYCHLEWSKI, The plane plastic strain problem of a wedge with jump non-homogeneity. *J. Mécanique* **3,** 461 (1964).
[3] J. RYCHLEWSKI, Plane plastic strain for jump non-homogeneity. *Int. J. Non-linear Mech.* **1,** 1 (1966).
[4] J. RYCHLEWSKI, Plastic torsion of bars with jump non-homogeneity. *Acta Mechanica* **1,** 36 (1965).
[5] J. RYCHLEWSKI, Plastic torsion of a rectangular bar with jump non-homogeneity *Int. J. Solids Struct.* **1,** 243 (1965).
[6] A. SAWCZUK and TH. JAEGER, *Grenztragfähigkeits-Theorie der Platten.* Springer (1963).
[7] A. SAWCZUK, Some problems of load carrying capacities of orthotropic and non-homogeneous plates. *Arch. Mech. Stosow.* **8,** 549 (1956). Also *IX-e Congres Int. de Mecanique Appliquee Actes* 8, Universite de Bruxelles, 1957, pp. 93–102.

(*Received* 20 *October* 1965)

Résumé—Dans plusieurs problèmes pratiques, le besoin se fait sentir de considerer les corps dont la non-homogénéité est decrite par des fonctions discontinues.

Le sujet de ce rapport est la determination de la capacité portante de plaques circulaires simplement supportées, soumises à une pression uniforme et composées de parties annulaire concentriques ayant des propriétés mécaniques differantes. Cette discontinuité des propriétés mécaniques peut etre causée par une discontinuité de l'épaisseur de la plaque ou par une discontinuité des propriétés du materiau.

Pour les plaques isotropes il y a six solutions différentes qui dependent des paramètres determinant la nonhomogéité et la division de la plaque. Dans chaque cas particulier on a trouvér les champs des moments, les champs des vitesses et la charge limite. L'éspace de validité de toutes les solutions est établi, le problème de la forme optimum dans la classe de ces plaques est également considéré.

La seconde partie s'occupe spécialement des plaques orthotropes, tout particulièrement d'une plaque en beton armé avec distribution uniforme de l'armature circoférentielle. Dans ce cas également, il y a sept solutions differentes qui dependent des parametres caracteristiques.

L'analyse ci-dessus a permi de tirer quelque conclusions qualitatives concernant la formation de plaques isotropes et orthotropes à nonhomogénéité discontinue.

Zusammenfassung—In vielen praktischen Fragen ist es notwendig, Körper, deren Nichthomogenität von unstetigen Funktionen beschrieben ist, zu betrachten.

Der Gegenstand dieser Abhandlung ist die Bestimmung der Grenztragfähigkeit der frei drehbar gestützten mit gleichmässigem Druck belasteten Kreisplatten, die aus konzentrischen ringförmigen Teilen von verschiedenen mechanischen Eigenschaften bestehen. Dieser Sprung der mechanischen Eigenschaften kann von einem Sprung der Plattendicke oder von einer plötzlichen Veränderung der Stoffeigenschaften verursacht werden.

Für das Problem der Grenztragfähigkeit einer isotropen Platte gibt es sechs verschiedene Lösungen, die von den Werten der Nichthomogenitäts- und Teilungsparametern abhängen. In jedem einzelnen Falle werden

Momenten- und Geschwindigkeitsfelder, Grenzlast sowie Gültigkeitsbereich der Lösung angegeben. Die Frage der optimalen Gestaltung von Platten der obigen Klasse wird auch untersucht.

Im zweiten Teil werden die orthotropen Platten erörtert. Als Sonderfall wird eine Stahlbetonplatte mit gleichmässiger Verteilung der Ringbewehrung betrachtet. Hier gibt es sieben verschiedene von Parameterwerten abhängige Lösungen.

Die durchgeführte Analyse gestattet gewisse qualitative Schlüsse über die Gestaltung der isotropen und orthotropen Platten von unstetiger Nichthomogenität.

Абстракт—Многие прикладные задачи приводят к необходимости рассмотрения тел, неоднородность которых описывают разрывные функции.

Предметом настоящей статьи является определение несущей способности свободно опертых круглых пластинок, состоящих из концентрических кольцевых частей различной прочности, нагруженных равномерным давлением. Скачок прочности может быть нызван скачком толщины или скачком механических свойств материала.

В зависимости от значений параметра неоднородности и параметра деления, задача о несущей способности изотропной пластинки имеет шесть различных решений. Для каждого случая указаны распределения моментов, скорости прогиба а также предельная нагрузка. Даны пределы применимости полученных решений. Обсуждается задача о оптимальной форме пластинки рассматриваемого класса.

Во второй части изучаются ортотропные пластинки. Обсуждается частный случай железобетонной пластинки с равномерно распределенной по лучу окружной армировкой. Здесь, в свою очередь, в соответствии со значениями параметров, имеется семь различных решений.

Проведенное исследование приводит к некоторым качественным выводам относительно проектирования изотропных и ортотропных пластинок с разрывной неоднородностью.